SUPPLEMENT

Figure S1 (related to Figure 1): Supporting cryo-EM data.

A. Representative micrographs for APCΔ7 apoenzyme (left) or holoenzyme (right).
B. Representative 2D classes for APCΔ7 apoenzyme (left) or holoenzyme (right).
C. Comparison of select 2D classes for wild-type APC (left, unpublished data in-house), and APCΔ7 apoenzyme (middle) or holoenzyme (right). The presence or absence of APC7 in this pose is indicated with a white arrow.
D. Gold-standard Fourier Shell Correlation traces for APCΔ7 apoenzyme (left) or holoenzyme (right). The 0.143 cutoff is indicated as a horizontal line, and values are available in Table S1.

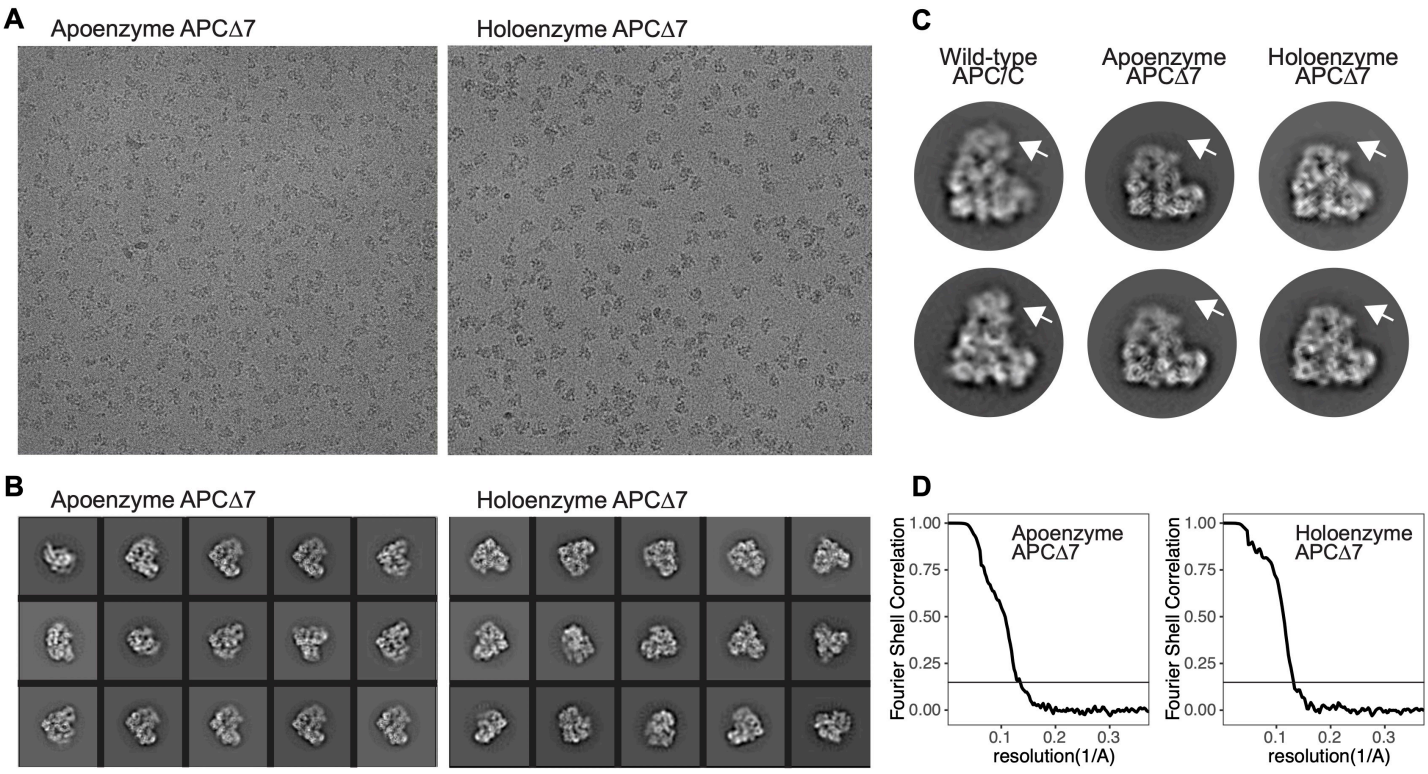
A
Apoenzyme APCΔ7
Holoenzyme APCΔ7
B
Apoenzyme APCΔ7
Holoenzyme APCΔ7
C
Wild-type APC/C
Apoenzyme APCΔ7
Holoenzyme APCΔ7
D
Fourier Shell Correlation
1.00
0.75
0.50
0.25
0.00
0.1
0.2
0.3
resolution(1/A)
Apoenzyme APCΔ7
Holoenzyme APCΔ7

Figure S2 (related to Figure 2): Loss of APC7 in the HAP1 cell line impairs substrate ubiquitination *in vitro*.

A. IP with anti-APC3 or isotype control antibody from HAP1 cell lysates followed by *in vitro* ubiquitination assays using the fluorescent substrates CycB-NTD and securin. Purified ubiquitin, Cdh1, E1 and E2 (Ube2C) were also included in the reaction.
B. IP of APC3 from HAP1 cell lysates followed by *in vitro* assessment of substrate ubiquitination by the E2 enzyme Ube2C.
C. IP of APC3 from HAP1 cell lysates followed by *in vitro* assessment of combined substrate ubiquitination (Ube2C) and ubiquitin chain elongation (Ube2S).
D. IP of APC3 from HAP1 cell lysates followed by *in vitro* assessment ubiquitination in response to escalating Ube2C. The reaction was stopped after 45 min.
E. IP of APC3 from HAP1 cell lysates followed by *in vitro* assessment of ubiquitination using escalating concentrations of the substrate-binding coactivator Cdh1. The reaction was stopped after 45 min.

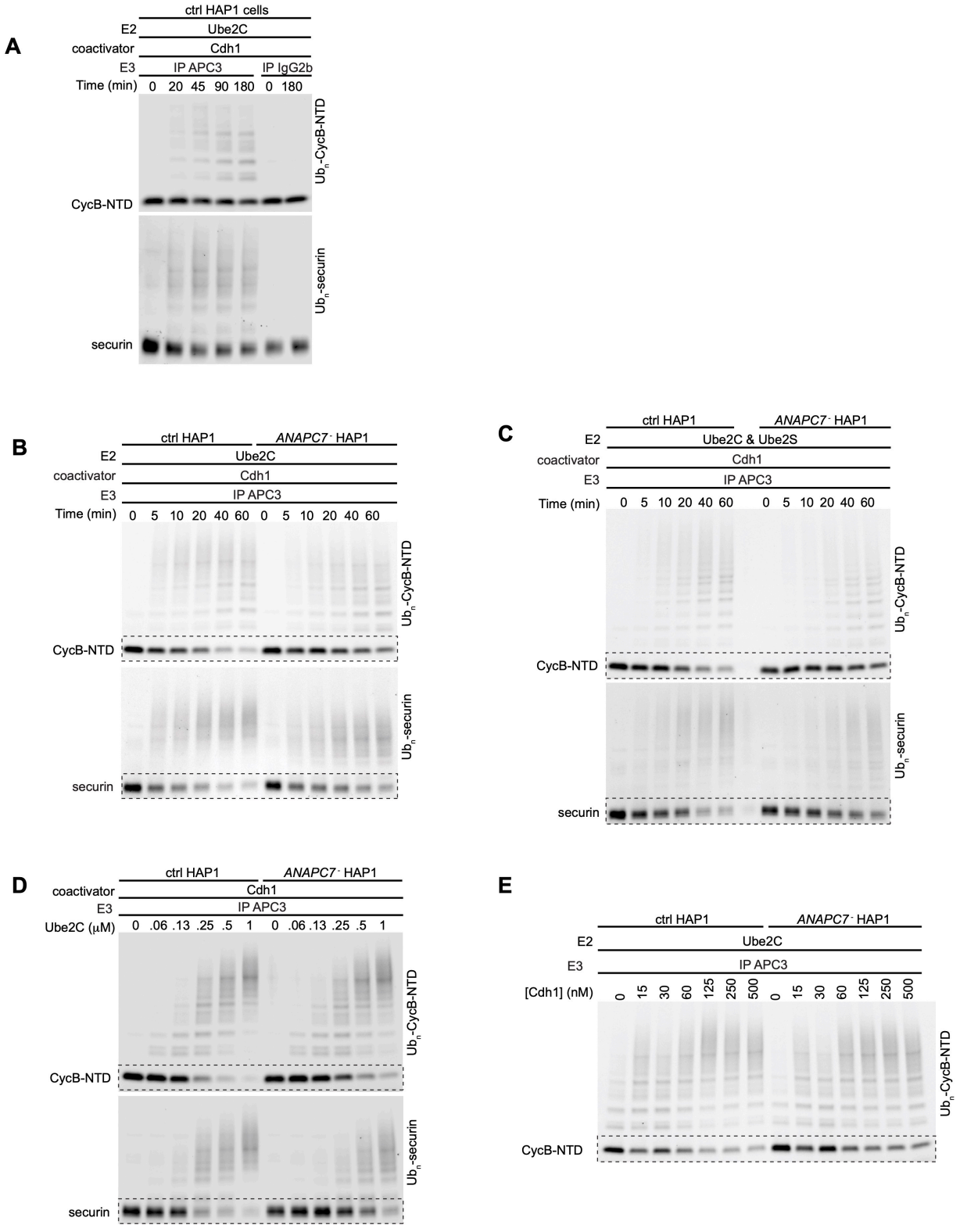
A
ctrl HAP1 cells
E2
Ube2C
coactivator
Cdh1
E3
IP APC3
IP IgG2b
Time (min)
0 20 45 90 180 0 180
Ub$_n$-CycB-NTD
CycB-NTD
Ub$_n$-securin
securin
B
ctrl HAP1
ANAPC7- HAP1
E2
Ube2C
coactivator
Cdh1
E3
IP APC3
Time (min)
0 5 10 20 40 60 0 5 10 20 40 60
Ub$_n$-CycB-NTD
CycB-NTD
Ub$_n$-securin
securin
C
ctrl HAP1
ANAPC7- HAP1
E2
Ube2C & Ube2S
coactivator
Cdh1
E3
IP APC3
Time (min)
0 5 10 20 40 60 0 5 10 20 40 60
Ub$_n$-CycB-NTD
CycB-NTD
Ub$_n$-securin
securin
D
ctrl HAP1
ANAPC7- HAP1
coactivator
Cdh1
E3
IP APC3
Ube2C (μM)
0 .06 .13 .25 .5 1 0 .06 .13 .25 .5 1
Ub$_n$-CycB-NTD
CycB-NTD
Ub$_n$-securin
securin
E
ctrl HAP1
ANAPC7- HAP1
E2
Ube2C
E3
IP APC3
[Cdh1] (nM)
0 15 30 60 125 250 500 0 15 30 60 125 250 500
Ub$_n$-CycB-NTD
CycB-NTD

Figure S3 (related to Figure 3): Genetic and clinical characterization of patients with the *ANAPC7* syndrome.

A. Array comparative genome hybridization (CGH) showing each patient's genotype at single nucleotide polymorphisms. Brown regions represent the maximum possible size for the deletion in *ANAPC7*.
B. Sequencing chromatogram of DNA from lymphoblasts of patient 2227. The deletion begins in intron 3 and ends in intron 6 of *ANAPC7*.
C. Pedigree connecting affected probands.
D. Body weight, length and head circumference of affected patients. Data shown as age and sex adjusted Z scores, where Z= [patient value – reference mean]/[one reference standard deviation].
E. Cumulative distribution of patients' ability to sit and walk independently as compared to unaffected controls (p-value by chi-square test).

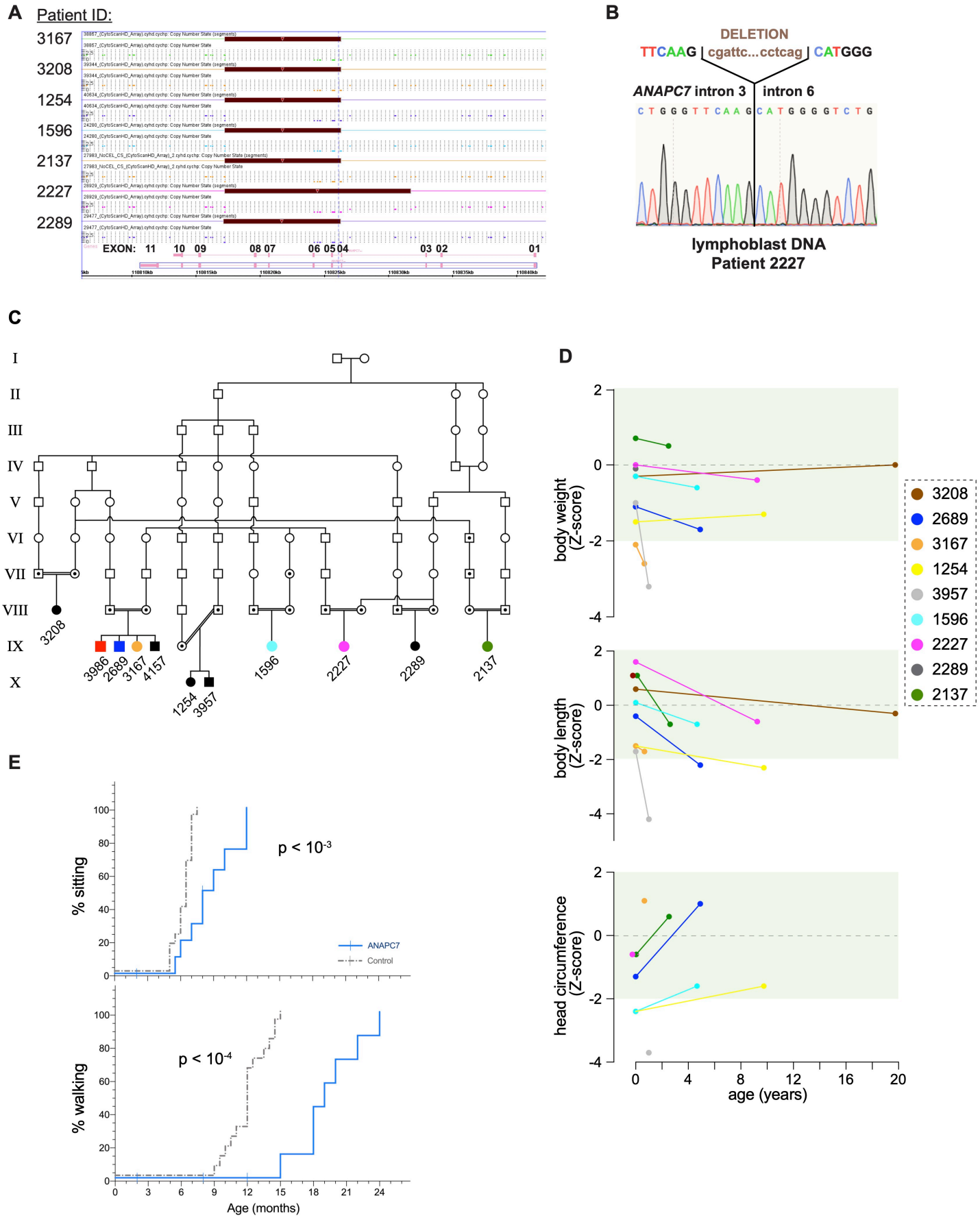
A
Patient ID:
3167
3208
1254
1596
2137
2227
2289
EXON: 11 10 09 08 07 06 05 04 03 02 01
B
DELETION
TTCAAG | cgattc...cctcag | CATGGG
ANAPC7 intron 3
intron 6
C T G G G T T C A A G C A T G G G G T C T G
lymphoblast DNA
Patient 2227
C
I
II
III
IV
V
VI
VII
VIII
IX
X
3208
3986
2689
3167
4157
1254
3957
1596
2227
2289
2137
D
body weight (Z-score)
body length (Z-score)
head circumference (Z-score)
2
0
-2
-4
0
4
8
12
16
20
age (years)
3208
2689
3167
1254
3957
1596
2227
2289
2137
E
% sitting
% walking
p < 10-3
p < 10-4
ANAPC7
Control
0
20
40
60
80
100
0
3
6
9
12
15
18
21
24
Age (months)

Figure S4 (related to Figure 3): APC7 is enriched in nuclei and APC abundance and enzymatic activity decline during mouse brain development.

A. IB of APC subunits from the TPR (tetratricopeptide repeat) lobe and platform sub-complexes over developmental time. Mechanical dissociation was used to separate whole brain into nuclear and cytoplasmic fractions. Boxed regions highlight the cellular distribution of APC7 and APC3, which are distinct from other APC subunits.
B. IB of APC subunits in the developing cerebral cortex in different cellular fractions.
C. IB of APC subunits in the developing cerebellum in different cellular fractions.
D. *In vitro* ubiquitination assay using immunoprecipitation of APC3 from whole brain as the source of E3 ubiquitin ligase. E1, Ube2C, Cdh1 and fluorescent cyclin B1-NTD (N-term domain) were included in the reaction.
E. Densitometry-based quantitation of the abundance of the unmodified substrate over time. Band were normalized to the amount of substrate at time 0 for a given biological sample. P-values reflect differences between a time point on one curve and the same time point on the curve lying above or below. Error bars SEM (N = 4, **p < 0.01, ***p <0.001, ****p<0.0001, by repeated measure ANOVA with Tukey test).

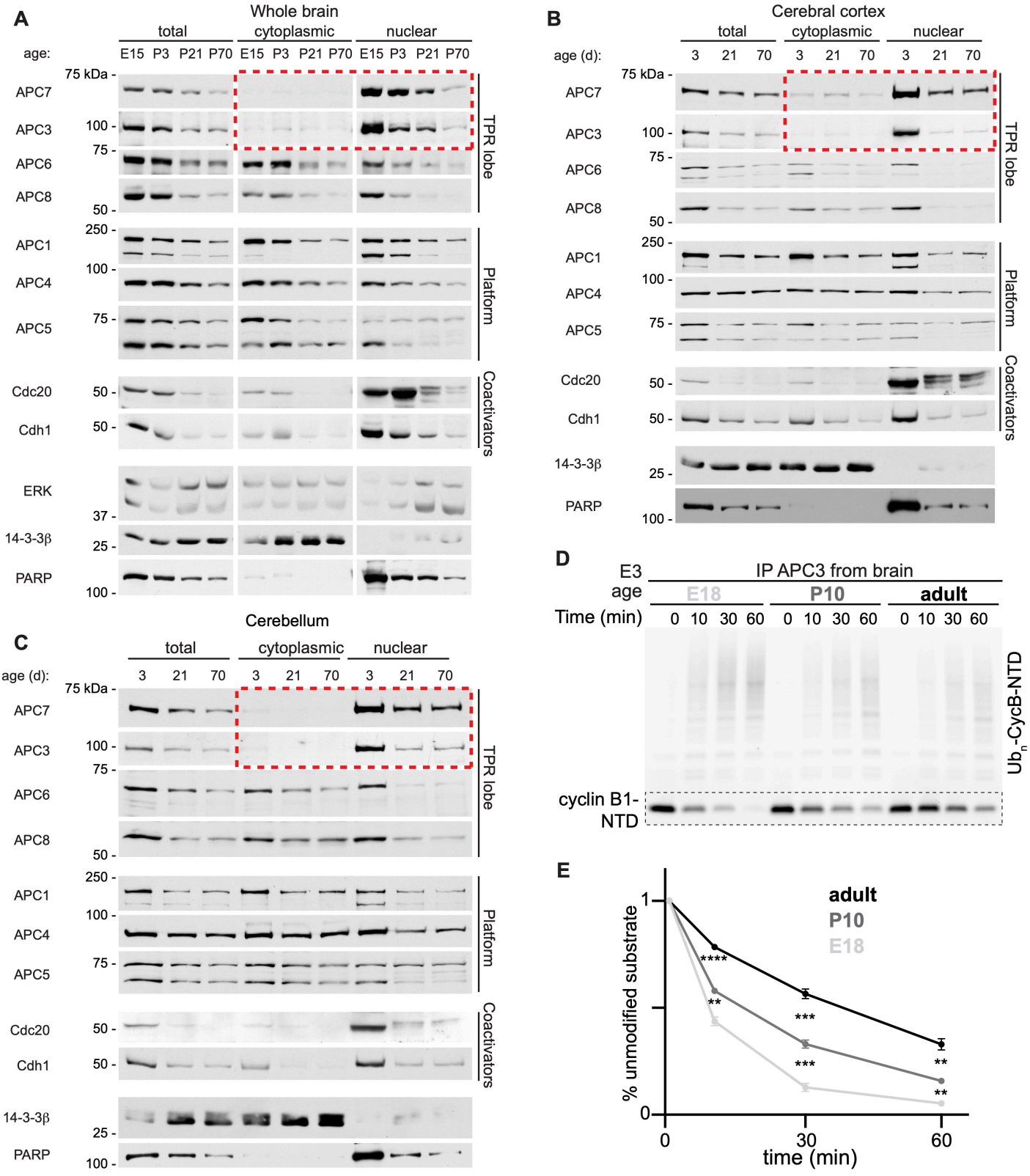
A
Whole brain
total
cytoplasmic
nuclear
age:
E15 P3 P21 P70 E15 P3 P21 P70 E15 P3 P21 P70
75 kDa
APC7
APC3
100
75
APC6
APC8
50
250
APC1
100
APC4
75
APC5
TPR lobe
Platform
Cdc20
50
Cdh1
50
Coactivators
ERK
37
14-3-3β
25
PARP
100
B
Cerebral cortex
total
cytoplasmic
nuclear
age (d):
3 21 70 3 21 70 3 21 70
75 kDa
APC7
APC3
100
75
APC6
APC8
50
250
APC1
100
APC4
75
APC5
TPR lobe
Platform
Cdc20
50
Cdh1
50
Coactivators
14-3-3β
25
PARP
100
C
Cerebellum
total
cytoplasmic
nuclear
age (d):
3 21 70 3 21 70 3 21 70
75 kDa
APC7
APC3
100
75
APC6
APC8
50
250
APC1
100
APC4
75
APC5
TPR lobe
Platform
Cdc20
50
Cdh1
50
Coactivators
14-3-3β
25
PARP
100
D
E3
IP APC3 from brain
age
E18
P10
adult
Time (min)
0 10 30 60 0 10 30 60 0 10 30 60
Ub_n-Cyclin B1-NTD
cyclin B1-NTD
E
adult
P10
E18
% unmodified substrate
1
0
0
30
60
time (min)
****
**
***
***
**
**

Figure S5 (related to Figure 3): Development and characterization of a knock-in mouse mutant that recapitulates the *ANAPC7* syndrome patient mutation.

A. Strategy for targeting of *Anapc7* by homologous recombination in mouse embryonic stem cells. The 565 amino acid sequence of mouse APC7 is 98% identical to human APC7, however an alternative start codon in humans leads to the addition of 34 amino acids at the N-terminus of human APC7. In mice and humans the mutant allele induces a frameshift in exon 7. The G>A mutation in exon 7 was added to the targeting vector to prevent the generation of a longer mistranslated portion of exon 7 in the mouse due to differences in DNA sequence between mouse and human.
B. Southern blot of the long arm of the targeting vector confirming successful recombination in clones 83, 32 and 42. Mice derived from blastocysts injected with clones 83 and 42 were selected for further study after establishing germline transmission in chimeric founders.
C. APC7 expression by RT-qPCR in primary cerebellar granule neurons at the indicated day *in vitro*. Error bars SEM (N = 4).
D. IP of endogenous APC1 and APC3 from mouse P5 whole brain followed by IB for components of the TPR lobe or the platform sub-complexes.
E. Mutant mice at the indicated day of embryonic development.
F. Growth of male and female mice through adulthood. Plots are staggered for display. Error bars SEM. No differences were observed at any age using repeated measures ANOVA and Tukey test.
G. H&E stained sections of the telencephalon at age E14 (LV, lateral ventricle; LGE, lateral ganglionic eminence). Cerebral cortex and hippocampal formation at age P7 (DG, dentate gyrus; WM, white matter). Cerebellum at P12.
H. Open field test. Error bars SEM (p-values by Kolmogorov-Smirnov test).

I. Elevated plus maze. Error bars SEM. No significant genotype effects by Kolmogorov-Smirnov test.

J. Sensorimotor battery of behavioral tests. Error bars SEM (p-values by Kolmogorov-Smirnov test).

K. Morris water maze. Error bars SEM (*$p < 0.04$ by repeated measure ANOVA with Bonferroni test).

L. Cued fear conditioning. Error bars SEM. No significant genotype effect by repeated measure ANOVA.

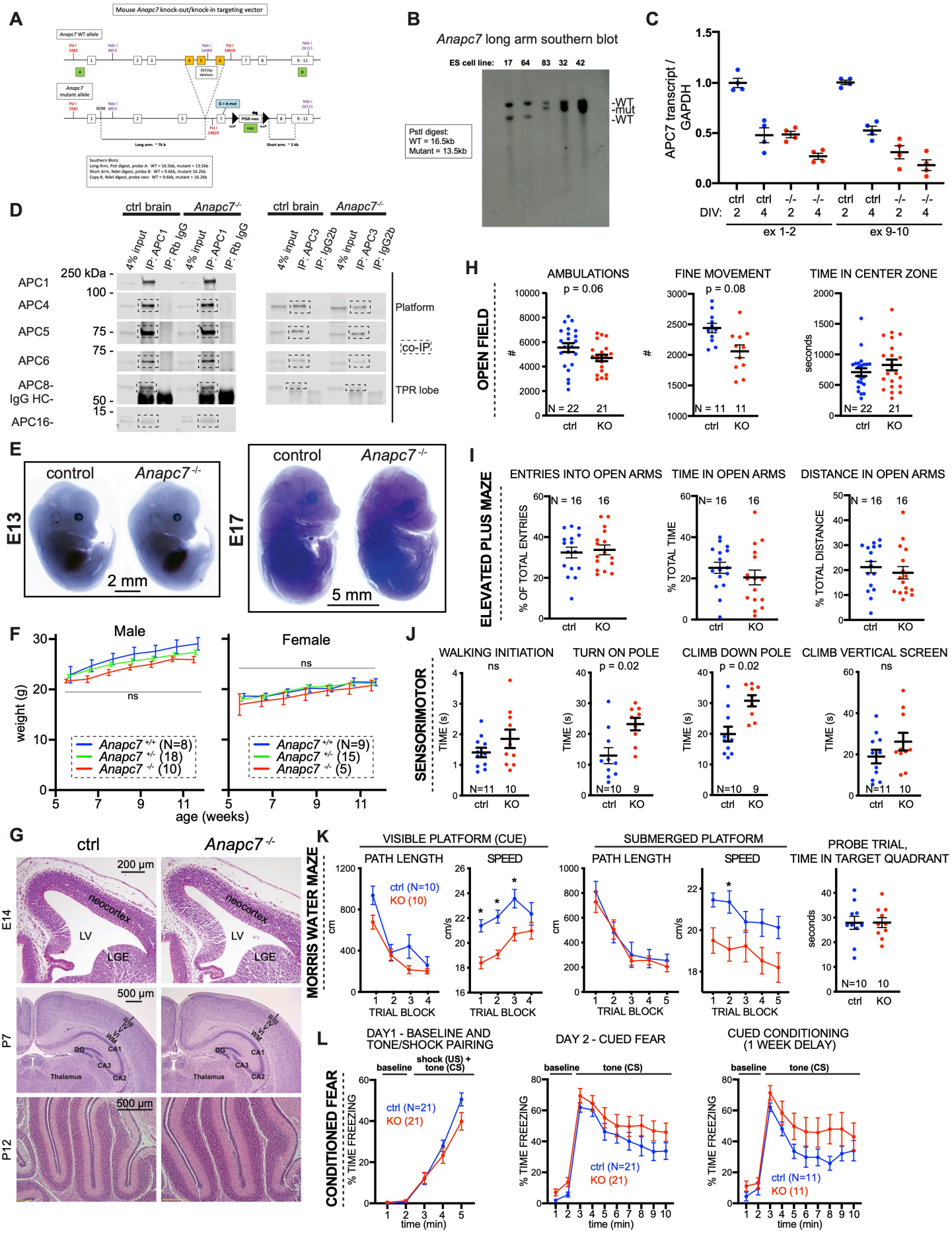
A
Mouse Anapc7 knock-out/knock-in targeting vector
Anapc7 WT allele
Anapc7 mutant allele
Southern Blots:
Long Arm, PstI digest, probe A: WT = 16.5kb, mutant = 13.5kb
Short Arm, NdeI digest, probe B: WT = 9.6kb, mutant 16.2kb
Copy #, NdeI digest, probe neo: WT = 9.6kb, mutant = 16.2kb
B
Anapc7 long arm southern blot
ES cell line: 17 64 83 32 42
PstI digest:
WT = 16.5kb
Mutant = 13.5kb
-WT
-mut
-WT
C
APC7 transcript / GAPDH
DIV:
ex 1-2
ex 9-10
D
ctrl brain
Anapc7-/-
4% input
IP: APC1
IP: Rb IgG
IP: APC3
IP: IgG2b
250 kDa
APC1
APC4
APC5
APC6
APC8-
IgG HC-
APC16-
Platform
co-IP
TPR lobe
E
control
Anapc7-/-
E13
E17
2 mm
5 mm
F
Male
Female
weight (g)
age (weeks)
Anapc7 +/+ (N=8)
Anapc7 +/- (18)
Anapc7 -/- (10)
Anapc7 +/+ (N=9)
Anapc7 +/- (15)
Anapc7 -/- (5)
ns
G
ctrl
Anapc7-/-
E14
P7
P12
200 µm
500 µm
neocortex
LV
LGE
DG
CA1
CA3
CA2
Thalamus
H
OPEN FIELD
AMBULATIONS
p = 0.06
FINE MOVEMENT
p = 0.08
TIME IN CENTER ZONE
#
seconds
N = 22
21
N = 11
11
ctrl
KO
I
ELEVATED PLUS MAZE
ENTRIES INTO OPEN ARMS
TIME IN OPEN ARMS
DISTANCE IN OPEN ARMS
% OF TOTAL ENTRIES
% TOTAL TIME
% TOTAL DISTANCE
J
SENSORIMOTOR
WALKING INITIATION
TURN ON POLE
p = 0.02
CLIMB DOWN POLE
p = 0.02
CLIMB VERTICAL SCREEN
TIME (s)
N=11
10
N=10
9
K
MORRIS WATER MAZE
VISIBLE PLATFORM (CUE)
SUBMERGED PLATFORM
PROBE TRIAL,
TIME IN TARGET QUADRANT
PATH LENGTH
SPEED
cm
cm/s
ctrl (N=10)
KO (10)
TRIAL BLOCK
L
CONDITIONED FEAR
DAY1 - BASELINE AND
TONE/SHOCK PAIRING
DAY 2 - CUED FEAR
CUED CONDITIONING
(1 WEEK DELAY)
baseline
shock (US) +
tone (CS)
tone (CS)
% TIME FREEZING
time (min)
ctrl (N=21)
KO (21)
ctrl (N=11)
KO (11)

Figure S6 (related to Figure 4): Loss of APC7 in the developing mouse brain does not perturb the cell cycle or neuronal migration.

A. Two-hour BrdU pulse at embryonic day 16 (E16) followed by IF detection of BrdU-positive cells in S phase. Positive cells in the developing isocortex were found in the ventricular zone (VZ) and sub-ventricular zone (SVZ) but not the cortical plate (CP).
B. Two-hour BrdU pulse at E15 followed by IF detection of BrdU in the VZ and SVZ of the telencephalon.
C. PCNA staining at E16 in the brainstem in the region of the 4th ventricle.
D. H3S10ph IF in P11 cerebellum.
E. Cyclin B1 IF in the region of the lateral ventricle at E16.
F. BrdU injection at P7 followed by IF detection of BrdU-labeled cells at P9 to assess migration into the internal granule layer (IGL).
G. BrdU injection at E17 followed by IF detection of BrdU-labeled cells at P7 to assess long-range migration into the superficial cortical layers.

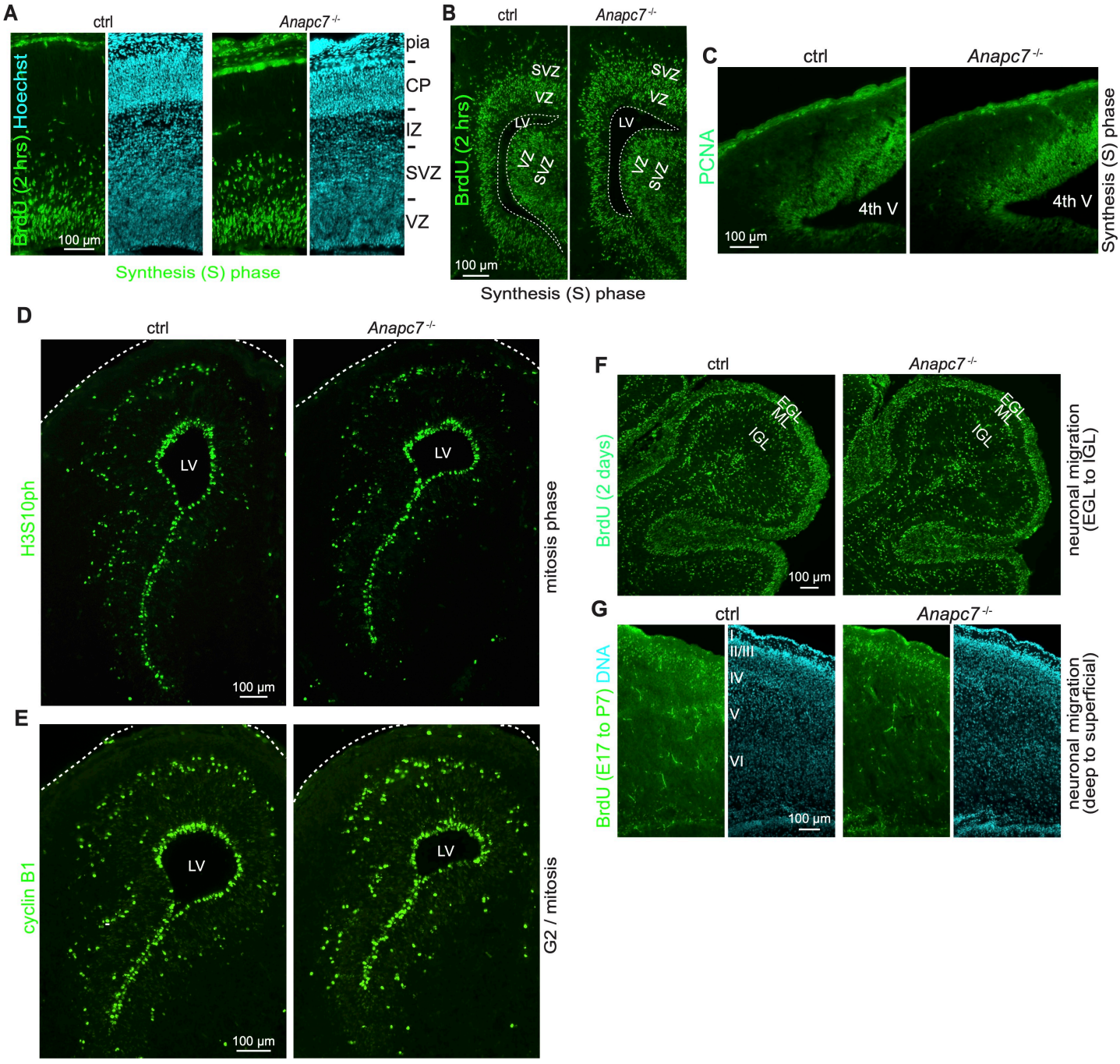
A
ctrl
Anapc7 -/-
BrdU (2 hrs),Hoechst
100 µm
pia
CP
IZ
SVZ
VZ
Synthesis (S) phase
B
ctrl
Anapc7 -/-
BrdU (2 hrs)
SVZ
VZ
LV
100 µm
Synthesis (S) phase
C
ctrl
Anapc7 -/-
PCNA
4th V
100 µm
Synthesis (S) phase
D
ctrl
Anapc7 -/-
H3S10ph
LV
100 µm
mitosis phase
E
cyclin B1
LV
100 µm
G2 / mitosis
F
ctrl
Anapc7 -/-
BrdU (2 days)
EGL
ML
IGL
100 µm
neuronal migration
(EGL to IGL)
G
ctrl
Anapc7 -/-
BrdU (E17 to P7) DNA
I
II/III
IV
V
VI
100 µm
neuronal migration
(deep to superficial)

Figure S7 (related to Figure 5): Ki-67 protein accumulates in post-mitotic neurons across the developing mutant brain.

A. Confocal IF of Ki-67 in the outer (o) and inner (i) external granule layer (EGL) of the cerebellum at P11.
B. Ki-67 IF at E18 in coronal sections of developing isocortex.
C. Ki-67 IF at E16 in coronal sections of the developing telencephalon (LGE, lateral ganglionic eminence; LV, lateral ventricle; ctx, cerebral cortex).
D. Ki-67 IF at E16 in the developing diencephalon with magnified areas.
E. Ki-67 IF at E16 in the developing brainstem with magnified areas.
F. Ki-67 IF at E16 in the brainstem in the region of the 4th ventricle.
G. Gating strategy for diploid nuclei labeled with anti-Ki-67 and Hoechst. Boxes represent gated regions depicted in the histogram in Figure 5I.
H. Ki-67 IB in primary granule neurons at the indicated day *in vitro*.
I. Densitometry-based quantitation of Ki-67 IB in primary granule neurons cultures at the indicated day *in vitro*. Error bars SEM (N = 3, p-values by two-way ANOVA and Bonferroni test).
J. Ki-67 RT-qPCR normalized to GAPDH in cultured primary granule neurons at the indicated DIV (N = 4).
K. Validation of a mouse line with RFP knocked in at the C-terminus of the endogenous *MKi67* locus (Ki-67-RFP). Anti-RFP resin was used to IP Ki67-RFP from benzonase-digested lysates of P7 cerebellum of the indicated genotypes. Anti-RFP IP pulled down Ki-67, which was detected by IB, only when the transgene was present.
L. Anti-RFP IP from benzonase-digested P8 cerebellar lysates from experimental *Anapc7*$^{-/-}$,Ki-67-RFP and control *Anapc7*$^{+/+}$,Ki-67-RFP mice.
M. Detection of Ki-67-RFP by confocal microscopy in DIV2 primary granule neurons from mice of the indicated genotypes.

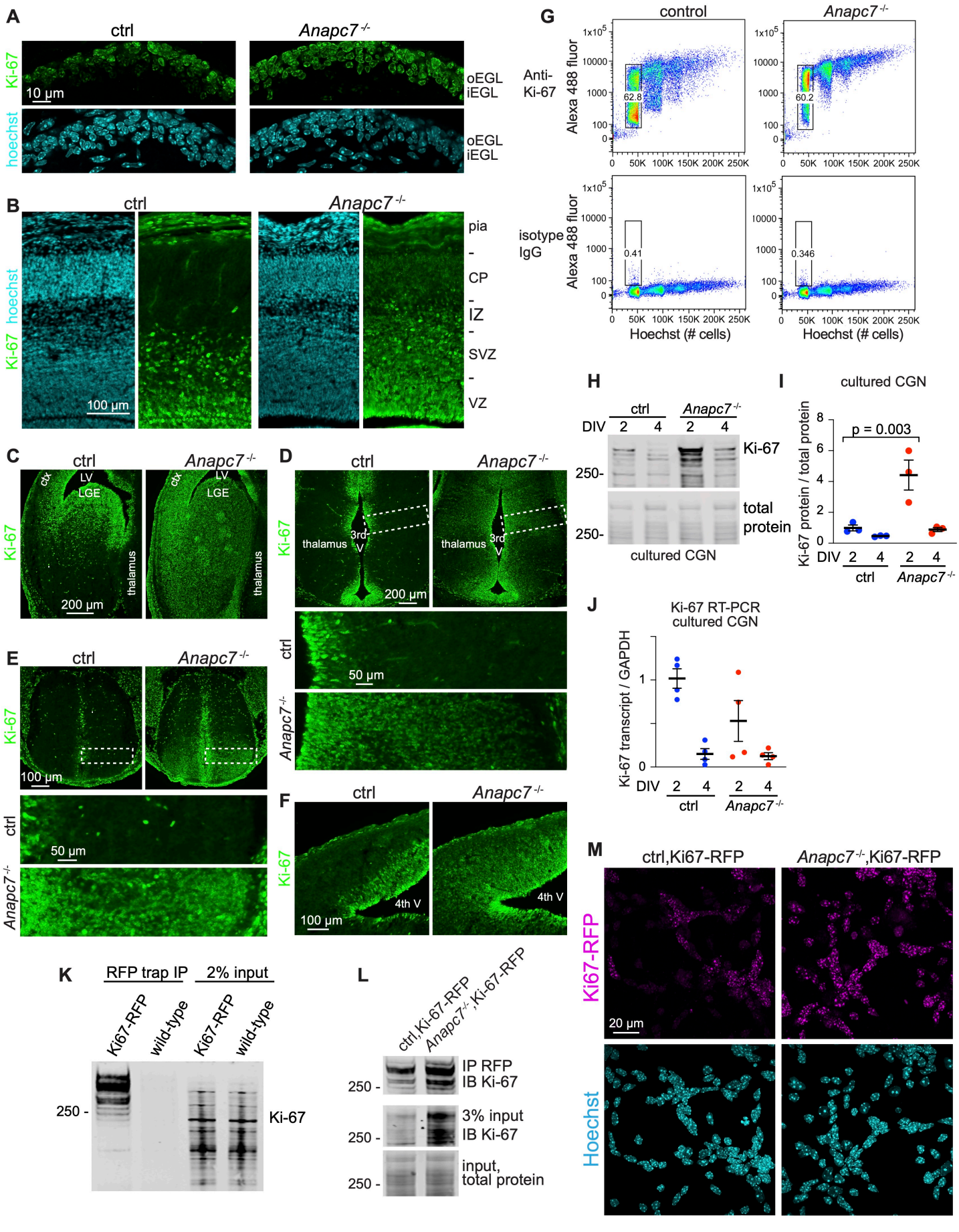
A
ctrl
Anapc7 -/-
Ki-67
hoechst
10 µm
oEGL
iEGL
B
pia
CP
IZ
SVZ
VZ
100 µm
C
ctx
LV
LGE
thalamus
200 µm
D
3rd V
E
100 µm
50 µm
F
4th V
G
control
Anti-Ki-67
isotype IgG
Alexa 488 fluor
62.8
60.2
0.41
0.346
Hoechst (# cells)
H
DIV 2 4 2 4
Ki-67
total protein
cultured CGN
I
cultured CGN
p = 0.003
Ki-67 protein / total protein
J
Ki-67 RT-PCR
cultured CGN
Ki-67 transcript / GAPDH
K
RFP trap IP
2% input
Ki67-RFP
wild-type
250 -
L
ctrl,Ki-67-RFP
Anapc7-/-;Ki-67-RFP
IP RFP
IB Ki-67
3% input
input, total protein
M
ctrl,Ki67-RFP
Anapc7-/-,Ki67-RFP
Ki67-RFP
Hoechst
20 µm

SUPPLEMENTAL TABLES

Table S1 (related to Figure 1): Cryo-EM imaging and data processing statistics

Table S2 (related to Figure 3): Clinical characteristics of patients with the *ANAPC7* syndrome

Table S4 (related to STAR Methods): Oligonucleotides used in this study

Table S1 (Related to Figure 1): Cryo-EM imaging and data processing statistics

	APCΔ7	APCΔ7-Cdh1-Ube2c-UbV
Microscope	Titan Krios	Titan Krios
Magnification	105,000	105,000
Voltage	300	300
Electron exposure e−/A^2	60	57
Defocus range (μm)	-1.2 ~ -3.6	-0.7 ~ 3.4
Pixel Size (A˚)	1.34	1.34
Symmetry Imposed	C1	C1
Initial particle Images (nos)	1,736,614	305,406
Final particle images (nos)	113,895	54,172
Map Resolution (A˚)	7.4	7.6
FSC threshold	0.143	0.143
Alignment Accuracy		
Rotation (°)	2.1	2.5
Translation (pixels)	1.2	1.6

Table S2 (Related to Figure 3): Clinical characteristics of patients with the *ANAPC7* syndrome

	Family 1	Family 2				Family 3		Family 4	Family 5	Family 6	Family 7
Patient ID	3208	3986	2689	3167	4157	1254	3957	1596	2227	2289	2137
Sex	F	M	M	F	M	F	M	F	F	F	F
Indication for Referral	Primary Amenorrhea	Incidentally seen with sibling	Poor weight gain	Developmental delay	Family history of *ANAPC7* deletion	Cleft palate, Developmental delay	Diaphragmatic hernia	Developmental delay	Developmental Delay	Intellectual Disability	Developmental delay
Age at last evaluation	19y 9m	3y 5m	4y 11 m	8m	2m	9y 9m	12 m	4y 8m	9y 3m	18y 10m	2y 6m
Craniofacial			m								
Micrognathia	-	-	+	-	+	+	+	+	-	-	+
High-arched palate	-	-	+	+					-		+
Cleft palate	-	-	-	-	-	+	+	-	-	-	-
Strabismus	+	+	-	-		+	+	-	+	-	-
Hearing loss	-	+	+	+		+		-	-	-	+
Hypertelorism	-	+	+	+		+	+	+	-	-	-

Neurologic											
Developmental delay/ Intellectual disability	+	+	+	+		+	+	+	+	+	+
Hypotonia	-	+	+	+		-	+	+	+	+	+
Skeletal											
Pectus Excavatum	-	+	+	+		+	-	-	+	+	+
Other	unilateral Congenital hypertrophy of the retinal pigment epithelium, primary ovarian failure		unilateral coronal suture ridge, coronary to pulmonary artery fistula			bilateral stenotic ear canals	Congenital diaphragmatic hernia, unilateral ptosis, microcephaly, patent foramen ovale				

Table S3 (Related to Figure 5): Tandem-mass tag (TMT) proteomics in control and *Anapc7*$^{-/-}$ cerebellum at P8. Data available in the attached excel spreadsheet.

Table S4 (Related to STAR methods): Oligonucleotides used in this study

APC7 ex 1-2 RT-PCR – F primer GTGATAGACCACGTGCGG	This paper	N/A
APC7 ex 1-2 RT-PCR – R primer TTCTGCGACGGGGAAAACAG	This paper	N/A
APC7 ex 3-5 RT-PCR – F primer TGCTGTACTCGATGGGATCC	This paper	N/A
APC7 ex 3-5 RT-PCR – R primer CGTCATTGATGCCACCTCTG	This paper	N/A
APC7 ex 9-10 RT-PCR – F primer TTGTCGCTTGGACTGTTACG	This paper	N/A
APC7 ex 9-10 RT-PCR – R primer TCCTGGGTCACTGGATCTTC	This paper	N/A
Ki-67 RT-PCR - F primer AATCCAACTCAAGTAAACGGGG	(Sobecki et al., 2016)	N/A
Ki-67 RT-PCR - R primer TTGGCTTGCTTCCATCCTCA	(Sobecki et al., 2016)	N/A
GAPDH RT-PCR - F primer GTTGTCTCCTGCGACTTCA	This paper	N/A
GAPDH RT-PCR - R primer GGTGGTCCAGGGTTTCTT	This paper	N/A
Anapc7 genotype - F primer AGAATAGTAGTCGGGCATCAAATGAGCGCG	This paper	N/A
Anapc7 genotype - R1 primer TGGTGAAGAGCACTTGCTGGTCTTGCAGAG	This paper	N/A
Anapc7 genotype - R2 primer CTCTGACTTCCAAGAGCACCTGTCCTCACC	This paper	N/A
ANAPC7 CRISPR guide RNA #1 GCTGGCAAACCTGTACAAGA	This paper	N/A
ANAPC7 gRNA #1 – F primer AATGTACAGGCAAGATTGAGAAC	This paper	N/A
ANAPC7 gRNA #1 – R primer TTGCACAGGGTTGTGGGTAG	This paper	N/A
ANAPC7 CRISPR guide RNA #2 TCAGCATGCAGAACCGTGGG	This paper	N/A
ANAPC7 gRNA #2 – F primer GGTTCAAGCAATCCACCTGT	This paper	N/A
ANAPC7 gRNA #2 – R primer GAGCCTGTGATGGTGGAAAG	This paper	N/A
ANAPC7 CRISPR guide RNA #3 TGAATGTGATAGACCACGTG	This paper	N/A
ANAPC7 gRNA #3 – F primer GGATTCAGCCTAGCGATGTG	This paper	N/A
ANAPC7 gRNA #3 – R primer AAAGGCCGTTAGGTCTGTCC	This paper	N/A
ANAPC7 CRISPR guide RNA #4 TGCTGTGAGTAAGTATACCA	This paper	N/A
ANAPC7 gRNA #4 – F primer TGTGCAGCCTGGTTCCTAAC	This paper	N/A
ANAPC7 gRNA #4 – R primer GGGAGCTTGGATTGAAAGG	This paper	N/A
Fzr1,Cdh1 floxed allele genotyping – F primer GCTGGGGGACTTCTCATTTTCC	(García-Higuera et al., 2008)	N/A

Fzr1,Cdh1 floxed allele genotyping – R primer AGCATCGTGACCGCTTCACC	(García-Higuera et al., 2008)	N/A
Cdc20 floxed allele genotyping – F primer GATTTGCACTCACTGCTTCAACTGG	(Manchado et al., 2010)	N/A
Cdc20 floxed allele genotyping – R primer CTTTCTGATGCTCCTGAAATACACG	(Manchado et al., 2010)	N/A
Math1/Atoh1 cre genotyping – F primer CATTTAACACCGTCGTCACC	This paper	N/A
Math1/Atoh1 cre genotyping – R primer GCAAACGGACAGAAGCATTT	This paper	N/A
Major satellite – F primer GGCGAGAAAACTGAAAATCACG	(Ebert et al., 2013)	N/A
Major satellite – R primer AGGTCCTTCAGTGTGCATTTC	(Ebert et al., 2013)	N/A
LINE-1 – F primer CAATCGCGTGGAACTTGAGAC	(Skene et al., 2010)	N/A
LINE-1 – R primer GACTCAGCTGGCAAGGTAGC	(Skene et al., 2010)	N/A
IAP – F primer GCTTTCGTTTTTGGGGCTTGG	(Skene et al., 2010)	N/A
IAP – R primer CTTACTCCGCGTTCTCACGAC	(Skene et al., 2010)	N/A